# Morphological Dilation as Fractal Scaling in Roughness Measurement

**Peter Bakucz**

Óbuda University, Institute of Mechatronics and Vehicle Engineering
Népszínház u. 8, 1081 Budapest, Hungary
e-mail: bakucz.peter@bgk.uni-obuda.hu

**Rolf Krüger-Sehm**

Physikalisch-Technische Bundesanstalt (PTB), Fachbereich 5.1
Bundesallee 100, 38116 Braunschweig, Germany
e-mail: rolf.krueger-sehm@ptb.de

*Abstract: In this work we propose, that the morphological dilation acts as fractal filters rebuilding white noise roughness surfaces into fractal 1/fm noise surfaces. The fractality indicates that the dilation does not have characteristic length scale, and the structuring element follows power-law distribution. Yashchuk's binary pseudo-random grating standard has been dilated with spherical and free form tips between 50 nm and 2000 nm and two scaling regions are referred to the tip diameter versus scaling exponent diagram. The first one in the smaller tip diameter region has a fast slope and the second one in the intermediate and larger tip diameter has a gradual slope. The results show that the dilated surfaces arise from the activity of at least two dynamical systems.*

*Keywords: Roughness; Morphological Filtering; Fractals*

# 1 Introduction

The roughness signal is constructed through the detection of an interaction between the tip apex and measurement surface features, thence the signal mainly affected by the tip-defined dynamical systems [1] [2] [3].

The real surface could be determined first by measuring the height distribution of the surface (tip convolution or morphological dilation) and second by deconvolving the tip effect with morphological erosion [4]. These processes provide the complete mathematical description of a fabrication procedure within the framework of the mathematical morphology [5]. However, an engineering

surface is an example of a specific structure in the sense that the profile of a surface is irregular, i.e. has no characteristic scale [6] [7].

The purpose of this work is to investigate the morphological dilation operation on the Yashchuk binary pseudo random grating white noise surface [8]. The inherent power spectral density of a white noise is an identical function, independent of spatial frequency. The fractal scaling behavior of the morphological dilation suggests that the operation is scale-free in the sense, that changing the lengthscale associated with dilation results also has a fractal scaling form. Comparing the power spectral densities of the dilated surface, shows how strong the dilation attenuates the surface on each length scales and additionally the structuring element can be characterized.

# 2 Power Spectra

Variations in the height of an engineering surface can be described with the periodogram, which is the square of the coefficients in a Fourier series representation and measures the average variation of the surface at different frequencies (Fig. 1). The periodogram can be computed for the entire surface at once, or segments of the surface can be averaged together to form the power spectral density (PSD). A widely used PSD is based on the covariance method [10].

If touching engineering surface points are uncorrelated, then the PSD will be constant as a function of wave number, i.e. white noise. If touching points are correlated relative to points far separated the PSD will be considerable at subordinate wavelengths and small short wavelengths [15] [16].

In this work we show, that the morphological dilation operation scales as fractal filter in which the white noise power spectrums are rebuilt into fractal $1/f^m$ spectrums. In $1/f^m$ signal, the spectral power of fluctuations is reversely balanced to their frequency. Surfaces referenced any $1/f^m$ scaling therefore fulfil a multiscale relationship, because fluctuations at any wavelength are engaged in large fluctuations at longer wavelengths, and these, in turn, are engaged in larger fluctuations on longer lengthscales.

# 3 An Approximate Power Function for Tip Distribution

We characterize the dilation with a 9 point's spherical tip and free form tips (9 and 12 points) (Fig. 1). The tip diameter is defined between the $0^{th}$ and the $9^{th}$ ($12^{th}$) points. We used 21 tips, diameters between 50 nm – 2000 nm.

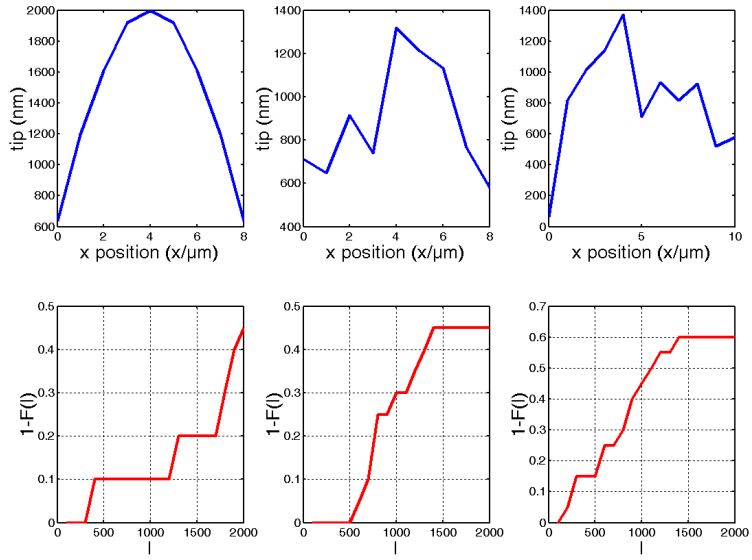


Figure 1
Spherical-, and 9-, 12 points free-form structuring elements (upper) and their distribution functions ($F(l)$)

The dilated surface points reflect the tip around the point weighted by their fractional contribution to the unfiltered input. Mathematically this means that the dilated output ($g_{dil}(n)$) at any value $n \in (0,1,...N)$ is the convolution of the input $g_{input}(n)$ and the tip $g_{tip}(l)$. ($l \in (-v,...,0,...v)$ $v$ is tip radius.)

$$g_{dil}(n) = \int_{-v}^{v} g_{tip}(l) g_{input}(n-l) dl = \max_{l=\{-v,...,v\}} \{g_{input}(n-l) + g_{tip}(l)\} \quad for \quad n = 0,1,..., N-2*v-2 \tag{1}$$

where $N$ is number of measured surface values.

From Eq (1) one can see, if the distribution of the tip is broad compared to the wavelength of the input surface, the filtering will be averaged but the fluctuations attenuated. The shorter the wavelength of the input compared to the tip distribution, the powerfuler this characterization by averaging processes. On the contrary, variations on length scales that are long related to the tip distribution will be transferred through the dilatation without meaningful extension.

By the convolution theorem, Eq (1) indicates

$$C_{dil}(f) = C_{tip}(f)C_{input}(f) \quad and \quad \left|C_{dil}(f)\right|^2 = \left|C_{tip}(f)\right|^2 \left|C_{input}(f)\right|^2 \quad (2)$$

Here $C_{dil}(f), C_{tip}(f), C_{input}(f)$ are the Fourier spectrums of $g_{dil}(l), g_{tip}(l)$ and $g_{input}(n-l)$ and $\left|C_{dil}(f)\right|^2, \left|C_{tip}(f)\right|^2, \left|C_{input}(f)\right|^2$ are their PSD. When the input surface is white noise, the $\left|C_{input}(f)\right|^2$ is approximately constant, and the PSD of the tip is roughly balanced to the PSD of filtered surface: $\left|C_{dil}(f)\right|^2 \propto \left|C_{tip}(f)\right|^2$.

The scaling behaviour, shown in (Fig. 2 right), is compatible with the assumption that the tip distribution power spectrum has a power decrease $\left|C_{tip}(f)\right|^2 \propto \frac{1}{f^m}$.

It is equally clear that this power decrease must break down for large *l*, because otherwise the tip distribution would become infinite.

An approximate distribution function *F(l)* that is integrable at large *l* could be expressed with the gamma function ($\Gamma()$):

$$F(l) = \frac{l^{\alpha-1}}{\beta^{\alpha}\Gamma(\alpha)} e^{-\frac{l}{\beta}} \quad (3)$$

where $\beta$ is a scale parameter and $\alpha = 1-m$ is a shape parameter [12].

Eq. 3. indicates a power spectrum of the form:

$$\left|C_{tip}(f)\right|^2 = (1+4\pi^2 f^2 \beta^2)^{-\alpha} \quad (4)$$

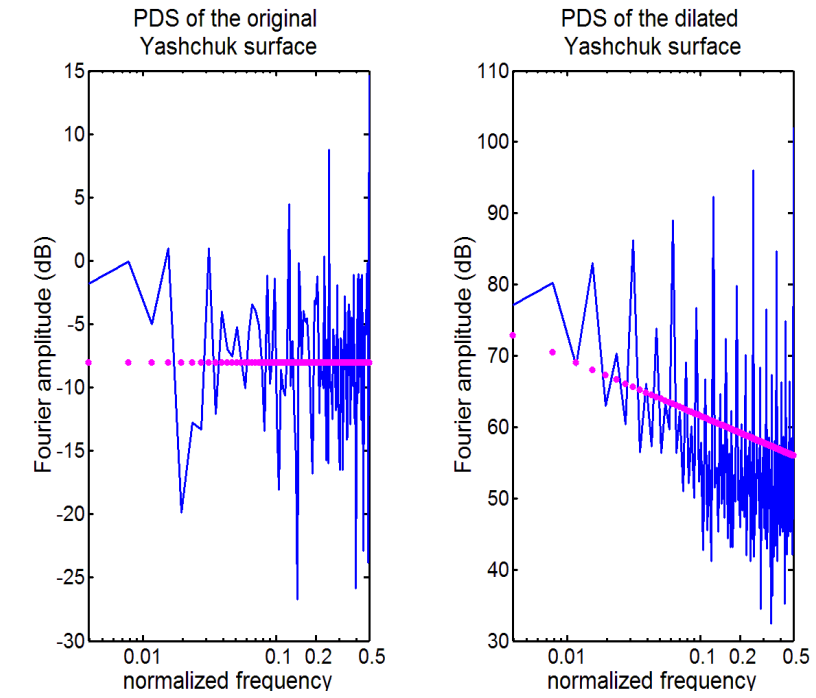


Figure 2

Binary pseudo-random grating standard (Yashchuk surface) of $2^8$ samples (normalized, left). Periodogram with least-squares fitting for the Yashchuk surface (middle), Periodogram with least-squares fitting for the 400 nm spherical tip dilated Yashchuk surface (right).

The PSD for the spherical-, and free-form 400 nm tips can be seen on Fig. 3. We used the exponential function fit (circle line) and Eq. (4) gamma function fit (star line) for the PSD signal (solid line). The PSD of the dilated surfaces with its fractal behavior could be better approximated by the gamma function. This is obviously the consequence of the localization of the gamma function, since the function "whiten" the surfaces. For the dilated surfaces at low frequencies the dilation operator behaves as a fractional differentiator.

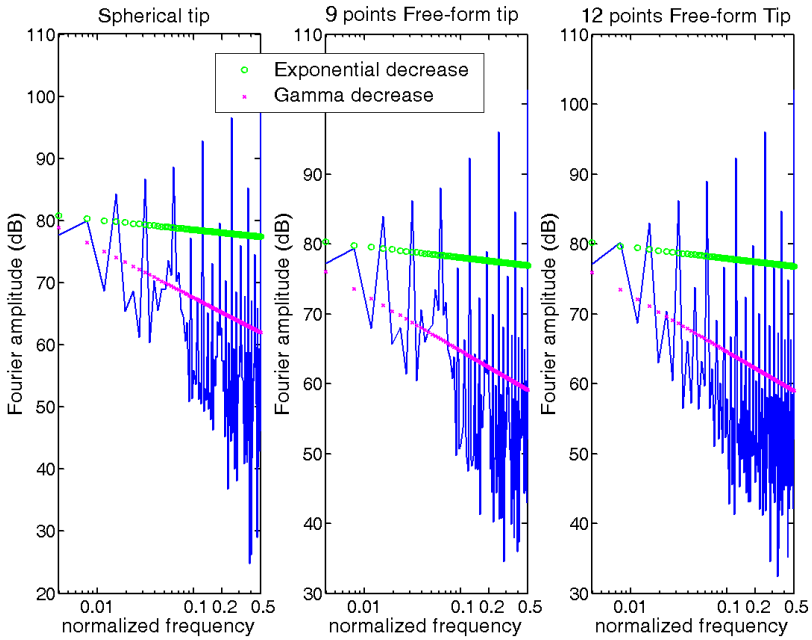


Figure 3

PSD of the dilated Yashchuk surface (solid line). Exponential function fit (circle line), gamma function fit (star line). The tip diameters are 400 nm.

# 4 Effects of Tipsize

It may be of interest to analyze the tip diameter corresponding the scaling parameter *m*.

Figure 4 is a plot of the relationship corresponding the scaling exponent and the tip diameter for spherical (solid line), 9 points free form (dashed line), and 12 points free form tips (dashdot line).

One can see two parts (scaling regions I and II) where the sign and the value of the slope are different. The slope of the lower region (300-700 nm for free form tips and 500-800 nm for spherical tip) decreases and the gradient of the upper region (700-2000 nm and 800-2000 nm) decreases as the tip diameter increases.

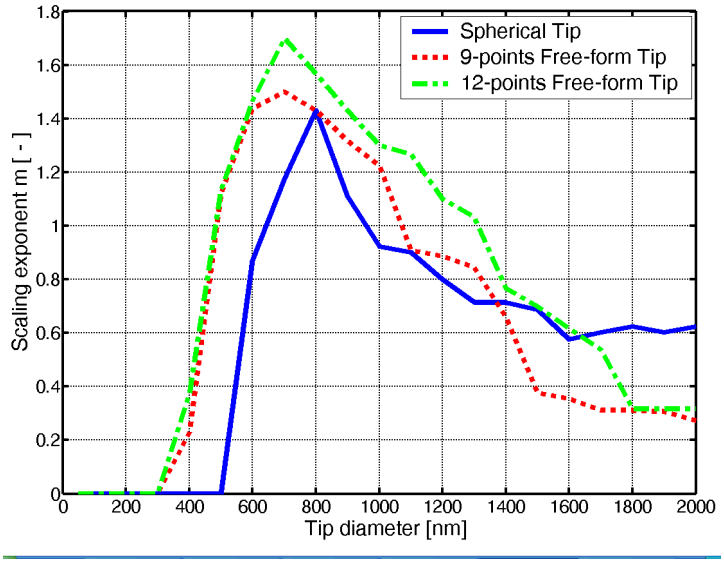


Figure 4

Scaling exponent vs. tip diameter relationship for spherical (solid line), 9 points free form (dotted line), and 12 points free form tips (dashdot line)

The scaling regions are result from the secular relation between nearby points of the surface and the points of the tip and the scaling regions are related to internal variations of Yashchuk surface.

In the Figure 5 the PSD of the two regimes are presented using covariance estimate. The similar scaling relations are observed for the free form tips.

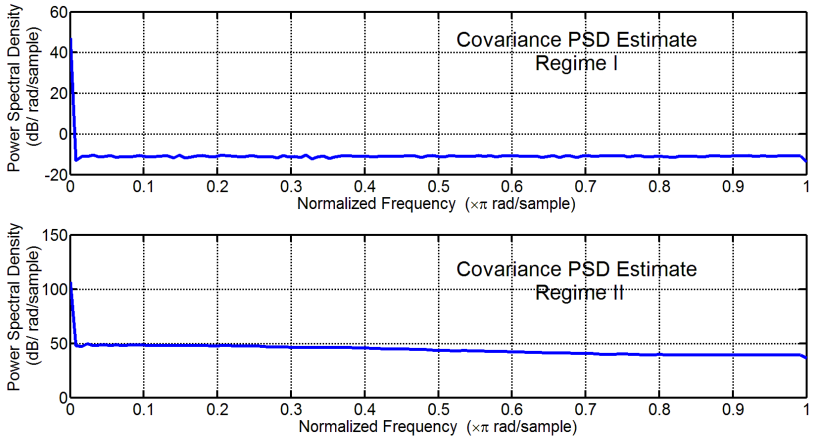


Figure 5

Covariance PSD of the two regimes dilated by 21 different spherical tips

The scaling regions have also been appeared in analyzing the dynamic of the dilated system with Kolmogorov entropy *K*. (Figure 6). The *K* describes a degree of chaoticity of system and gives the mean property of information loss about a phase point. In the statistical physics $K = 0$ in an deterministic space, *K* is infinite in a random space, and $0 < K < 1$ is in a chaotic space. (More detailed see in [13]).

For the scaling region I the slope of Kolmogorov entropy vs. tip diameter diagram of the dilated surfaces are between 0.27±0.09 and 0.15±0.06, respectively. In the scaling region I is the system chaotic.

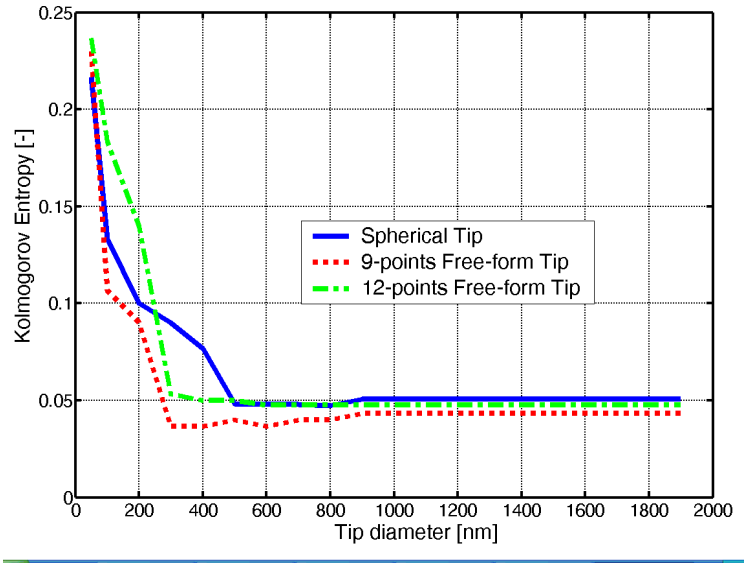


Figure 6

Kolmogorov Entropy for spherical (solid line), 9 points free form (dotted line), and 12 points free form tips (dashdot line)

The scaling region II with the constant near 0 slope in the scaling exponent system are revealed in the ranges of larger tip diameter. The information loss of this region shows that the system is fixed (Table 1).

Table 1

Slope of the Kolmogorov entropy vs. tip diameter diagram for the different scaling regions

| | scaling region I | scaling region II |
|---|---|---|
| Sperical tip | 0.27±0.09 | 0.05±0.001 |
| 9 points free form tip | 0.21±0.03 | 0.05±0.002 |
| 12 points free form tip | 0.15±0.06 | 0.04±0.002 |

## Conclusions

The affiliation between the PSD of the Yashchuk binary pseudo-random grating standard and the output dilated surfaces at each wavelength reflects how powerful the dilation changes the tip distribution space on each lengthscale. The power spectra of the dilated surfaces show fractal $1/f^m$ scaling; this indicates that dilation is acting as fractal filter, rebuilding the inputs into $1/f^m$ noise outputs with *m* scaling exponent. The scaling behaviour is directly related to the input standard lengthscale distribution. If the distribution is comprehensive to the wavelength of the tip distribution, then the fluctuation will be standardized and discouraged.

The relationship between the dilated signal and its PSD can be extracted, and the tip distribution can be determined. The fractal $1/f^m$ scaling is consistent with the tip distribution (*F(l)*) using the gamma function. The dilated tip PSD can present both long-term character of scans and short-term character to scans consequently the gamma distribution is an appropriate categorizing of the scaling behaviour and the tip distribution seen at the dilatation of the Yashchuk surface.

Analyzing the tip diameter versus scaling exponent diagram one can see two parts (scaling regions) where the sign and the value of the slope are different.

The scaling regions are result from the secular relation between nearby points of the surface and the points of the tip and the scaling regions are related to internal variations of Yashchuk surface:for the scaling region I is the system chaotic and the information loss of the scaling region II shows that the system here is already fixed [14].

## References

[1] Palásti-Kovács B, Néder Z, Czifra Á, Váradi K (2004) Microtopography Changes in Wear Process, in Acta Polytechnica Hungarica, Issue 1, No. 1

[2] Danzebrink H-U, Koenders L, Wilkening G, Yacoot A and Kunzmann H (2006) Advances in Scanning Force Microscopy for Dimensional Metrology *Ann. CIRP* **55** 841–79

[3] Fekete G, Horváth S, Czifra Á (2007) Microgeometry Tests of 'Contradictory' Surfaces with Various Evaluation Techniques, in Acta Polytechnica Hungarica, Issue 4, Number 4

[4] Giardina C. R. and Dougherty E. R. (1988) Morphological Methods in Image and Signal Processing. Englewood Cliffs, NJ, Prentice Hall

[5] Balagurunathan Y. and Dougherty E. (2003) Morphological Quantification of Surface Roughness. Opt. Eng. 42(6). 1795-1804

[6] Bakucz P. et al (2008) Influence of the Atomic Force Microscope Tip on the Multifractal Analysis of Rough Surfaces. Rev. of Scientific Instruments 79 073703

[7] Raja J. et al. (2002) Recent Advances in Separation of Roughness, Waviness and form. Precision Engineering. 5247. 1-14

[8] Yashchuk V. V., McKinney W. R. and Takács P. Z. (2007) Binary Pseudo-Random Grating as a Standard Test Surface for Measurement of Modulation Transfer Functions of Interferometric Microscopes. SPIE Optics and Photonics 2007 "Advances in Metrology for X-Ray and EUV Optics II" San Diego, August 30, 2007 Proceedings of SPIE 6704-7

[9] Brown C. A. and Savary G. (1998) Scale-Sensitivity, Fractal Analysis and Simulations. International Journal of Machine Tools and Manufacturing. 38. 5-6 1998. 633-637

[10] Marple, S. L (1987) *Digital Spectral Analysis*, Englewood Cliffs, NJ, Prentice-Hall, Chapter 7

[11] Stoica, P., and R. L. (1997) Moses, *Introduction to Spectral Analysis*, Prentice-Hall

[12] Bain, L. 1983: In Encyklopedia of Statistical Sciences. (ed. Kotz, S and Johnson , N. L.) 292-298. Wiley, New York

[13] Eckman J. and Ruelle, P. D. (1985) Ergodic Theory of Chaos and Strange Attractors Rev. Mod. Phys., 57, 617

[14] Dai G, Jung L., Pohlenz F., Danzebrink H. U., Krüger-Sehm R., Hasche K., and Wilkening G. (2004) Measurement of Micro Roughness Using a Metrological Large Range Scanning Force Microscope. Mes. Sci and Technology. 15. 2004. 2039-2046

[15] Czerkas S, Dziomba T and Bosse H 2005 Comparison of Different Methods of SFM Tip Shape Determination for Various Characterisation Structures and Types of Tip *Nanoscale Calibration Standards and Methods* ed G Wilkening and L Koenders (Weinheim: Wiley-VCH) ISBN 3-527-40502-X

[16] Yacoot A, Koenders L and Wolff H (2007) An Atomic Force Microscope for the Study of Tip Sample Interactions and their Effects on Dimensional Metrology *Meas. Sci. Technol.* **18** 350-9

[17] Binning G, Quate C F, Gerber C (1986) Atomic Force Microscope. *Physical Review Letters*. **56(9)**, 930-933

[18] Burnham N A, Colton R J (1989) Measuring the Nanomechanical Properties and Surface Forces of Materials Using an Atomic Force Microscope. *J. Vac. Sci. Technol* **A7**, 2134-2135

[19] Bushan, B. (2004) *Springer Handbook of Nanotechnology*. Springer